

Published in final edited form as:

Chem Asian J. 2012 November ; 7(11): 2592–2599. doi:10.1002/asia.201200488.

Selective detection of multi-carboxylate anions based on “turn on” electron-transfer by self-assembled molecular rectangles

Dr. Anurag Mishra^[a], Sunmi Lee^[a], Dr. Hyunuk Kim^[b], Dr. Timothy R. Cook^[c], Prof. Peter J. Stang^[c], and Prof. Ki-Whan Chi^[a]

Ki-Whan Chi: kwchi@ulsan.ac.kr

^[a]Department of Chemistry, University of Ulsan, Ulsan 680-749, Republic of Korea

^[b]Energy Materials and Convergence Research Department, Korea Institute of Energy Research, Daejeon 305-343, Republic of Korea

^[c]Department of Chemistry, University of Utah, Salt Lake City, Utah 84112, U.S.A

Abstract

Two new large molecular rectangles (**4** and **5**) were obtained by the reaction of two different dinuclear arene ruthenium complexes [Ru₂(arene)₂(OO \cap OO)₂Cl₂] [arene = *p*-cymene, OO \cap OO = 2,5-dihydroxy-1,4-benzoquinonato (**2**), 6,11-dihydroxy-5,12-naphthacene dionato (**3**)] with the unsymmetrical amide *MN* = *N*-(4-(pyridin-4-ylethynyl)phenyl) isonicotinamide donor ligand **1** in methanol in the presence of AgO₃SCF₃, forming tetranuclear cations of the general formula [Ru₄(arene)₄(*NN*)₂(OO \cap O O)₂]⁴⁺. Both rectangles were isolated in good yields as triflate salts and were characterized by multinuclear NMR, ESI-MS, UV–Vis and photo-luminescence spectroscopy. The crystal structure of **5** was determined by X-ray diffraction. The luminescent rectangle **5** was used for anion sensing with an amide ligand as a hydrogen bond donor and an arene-Ru acceptor as a signaling unit. Rectangle **5** strongly bound multi-carboxylate anions, such as oxalate, tartrate, and citrate, in UV–Vis titration experiments in 1:1 ratios in contrast to mono anions, such as F⁻, Cl⁻, NO₃⁻, PF₆⁻, CH₃COO⁻, and C₆H₅COO⁻. The fluorescence titration experiment showed a large fluorescence enhancement of **5** upon binding to multi-carboxylate anions, which can be attributed to the blocking of the photo-induced electron transfer (PET) process from the arene–Ru moiety to the amidic donor in **5** likely as a result of hydrogen bonding between the ligand and the anion. On the other hand, rectangle **5** was not selective towards any other anions. To the naked eye multi-carboxylate anions in a methanol solution of **5** appears greenish upon UV light irradiation.

Keywords

Self-assembled; amide ligand; ruthenium acceptor; anion sensing studies; multi-carboxylate anions

Introduction

Considerable efforts have been devoted to selectively sensing anions because of the important roles they play in various chemical, biological, and environmental sciences. ^[1, 2] Sensing multi-carboxylate anions is useful in chemistry as well as biochemistry. Of the multi-carboxylates, oxalate, citrate, and tartrate are particularly relevant for the detection of

Correspondence to: Ki-Whan Chi, kwchi@ulsan.ac.kr.

Supporting information for this article is available on the WWW under <http://dx.doi.org/10.1002/asia.200xxxxxx>.

several diseases, as they occur as intermediates in cellular metabolism.^[3] Excessive oxalate accumulation in the body can cause a variety of health disorders, such as renal failure,^[4] urinary stone disease,^[5] and pancreatic insufficiency.^[6] Citrate and tartrate are key metabolites in the Krebs cycle occurring in virtually every aerobic cell. Monitoring citrate levels is important to track clinical conditions and to assess normal cell metabolism. Diminished citrate levels in urine have been linked to various aspects of kidney dysfunction, for example the pathogenesis of nephrolithiasis and nephrocalcinosis.^[7] During the past decade, many artificial dicarboxylate sensors have been developed.^[8] There are few examples, however, of effective fluorescent sensors for multi-carboxylates.^[9] In general, receptors that tightly and selectively bind are challenging to develop for sensing purposes.^[10]

Selective chemosensors with anion-induced fluorescence have attracted particular attention because of their simplicity and high detection limits.^[11] Upon binding of a guest species, the photophysical characteristics of a receptor such as fluorescence intensity, emission wavelength, and fluorescence lifetime may change through various mechanisms, and such changes provide a signal to indicate binding.^[12] Commonly, a fluorophore is covalently linked to a receptor, which is designed to specifically recognize a target anion. The communication mechanism between receptor and fluorophore is frequently intramolecular photo-induced electron transfer (PET).^[13] Accordingly, a recognition event tunes the electronic properties of the receptor, which leads to either enhanced (turn-on) or reduced (turn-off) fluorescence by blocking or promoting PET, respectively.

Amide-containing groups are good H-bonding donors, and are used widely to design and synthesize artificial anion receptors.^[14] We previously reported that self-assembled metallabowls containing amides selectively sense dicarboxylate anions.^[15] Continuing that work, we report here the synthesis and anion sensing properties of new ruthenium-nitrogen based, self-assembled molecular rectangles. We previously reported the ligand used in this study,^[16] which was chosen taking several considerations into account. First, it includes central amide protons as hydrogen-bond donors which are expected to trap counter anions/guest molecules within the metalla-cycle *via* hydrogen bonding interactions.^[17] Second, terminal pyridine N donors are available to coordinate to metal ions which is a common motif in coordination-driven self-assembly.^[18] Third, the diaryl alkyne unit enforces structural rigidity, potentially enhancing the luminescent photo-physical properties by attenuating non-radiative vibrational decay pathways. Organometallic half-sandwich complexes based on ruthenium acceptors were chosen because of their precedent as effective building blocks for metallacycles and their prior demonstration of interesting electronic, structural, and signalling properties for sensors.^[19, 20]

In this paper, we describe the synthesis and characterization of two new molecular rectangles (**4** and **5**) with the general formulae $[\text{Ru}_4(\text{arene})_4(\text{OO}\text{N}\text{OO})_2(\text{N}\text{N}\text{N})_2]^{4+}$ (arene = *p*-cymene, OOONO = 2,5-dihydroxy-1,4-benzoquinonato (dhbq) (**4**), 6,11-dihydroxy-5,12-naphthacene dionato (dhnd) (**5**); *NNN* = *N*-(4-(pyridin-4-ylethynyl)phenyl) isonicotinamide, prepared from dinuclear complexes (**2** and **3**) and an unsymmetrical N-donor amide ligand (**1**; Scheme 1). In addition, we report the sensing behaviour of rectangle **5** with a variety of anions. Interestingly, rectangle **5** was highly selective and sensitive for multi-carboxylates, such as oxalate, tartrate, and citrate, while showing no significant response to monoanions, such as F^- , Cl^- , NO_3^- , PF_6^- , CH_3COO^- , $\text{C}_6\text{H}_5\text{COO}^-$, even when such anions were present in excess.

Results and Discussion

Synthesis and Characterization of Molecular Rectangles

When mixed at room temperature in methanolic solution, dinuclear ruthenium complexes $[\text{Ru}_2(\text{arene})_2(\text{OONO})\text{Cl}_2]$ (**2** and **3**) self-assemble with *N*-(4-(pyridin-4-ylethynyl)phenyl) isonicotinamide (**1**) to give molecular rectangles **4** and **5** stabilized as triflate salts (Scheme 1) when silver triflate is present as a halide scavenger. Precipitation via addition of diethyl ether yields **4** and **5** as analytically pure solids. Two isomeric molecular rectangles are possible, as depicted in Scheme 1.

The ^1H NMR spectra of both rectangles clearly showed two structural isomers with significant resonance shifts as compared to that of the free ligand, indicative of metal-ligand coordination.^[16] In the ^1H NMR spectra of rectangles **4** and **5**, these two isomers lead to two distinct sets of proton signals in the ratio of 1:1 (see Supporting Information S1 and S2). Furthermore, in rectangle **4** the two sets of signals are relatively broad while in **5** they are less broad and more defined. In the proton NMRs of both compounds, the α -H pyridine resonances moved upfield relative to the free ligand even though these protons are closest to the metal centers (see Supporting Information). This may result from ring current shielding, which offsets the downfield shift caused by metal induction.^[21]

The composition of the $[2 + 2]$ rectangular nature of **4** and **5** was supported by electrospray ionization mass spectrometry (ESI-MS). In the mass spectrum of assembly **4**, peaks at $m/z = 1057.1$ and 655.4 correspond to $[\text{M} - 2\text{OTf}]^{2+}$ and $[\text{M} - 3\text{OTf}]^{3+}$ charge states (Figure 1, upper) while the spectrum of **5** showed a peak at $m/z = 755.6$ corresponding to the $[\text{M} - 3\text{OTf}]^{3+}$ charge state (Figure 1, lower), all in good agreement with their theoretical isotopic distributions (Figure 1, blue).

The molecular structure of one isomer of **5** was unambiguously confirmed by single-crystal X-ray diffraction analysis. Crystals were obtained by the slow vapour diffusion of diethyl ether into a solution of **5** in a $\text{CH}_3\text{OH}/\text{CH}_3\text{NO}_2$ (1:1) solvent mixture. No ligand disorder was observed during refinement, indicating inclusion of only the *head-to-tail* isomer in the crystal whose structure is shown in Figure 2. Two dipyriddy ligands bridge two $[\text{Ru}_2(\text{arene})_2(6,11\text{-dihydroxy-}5,12\text{-naphthacene dio-nato})_2]^{4+}$ building blocks to form a $[2 + 2]$ M_4L_2 rectangle. Each cymene-capped Ru coordination sphere contains one nitrogen atom and two oxygen atoms which define the dipyriddy and naphthacene dionato vertices of the rectangle, respectively, resulting in a tetranuclear frame with internal dimensions of 4.4×16.5 Å. The Ru-N and Ru-O distances range between 2.038 and 2.179 Å, and are comparable to those found in known tetracationic rectangles.^[9a] Despite the head-to-tail binding of ligand **1** to the Ru centers, the amide group carbonyl (-CO-) and NH moieties aligned in the opposite direction.

Absorption and emission studies

The electronic absorption spectra of **4** and **5**, along with those of their corresponding metal acceptors (**2** and **3**) and donor ligand (**1**) were investigated using 1×10^{-5} M methanol solutions (Figure 3). The absorption spectra exhibit intense bands at $\lambda_{\text{abs}} = 317, 342$ and 500 nm for **4** and $\lambda_{\text{abs}} = 275, 332, 565,$ and 611 nm for **5**. The high-energy bands observed in both rectangles **4** and **5** were also present in the spectra of free ligand **1**. As such, these bands are likely due to $\pi \rightarrow \pi^*$ transitions of the ethynyl backbone which are preserved upon self-assembly. The dinuclear arene-Ru acceptors also exhibited high-energy absorption bands at 272–315 nm, as well as broad, low-energy absorption bands ranging from 480–600 nm. These bands are likely a combination of intra/intermolecular $\pi \rightarrow \pi^*$ transitions mixed with metal-to-ligand charge transfers. As with the pyridyl donor bands, these arene-Ru-

based bands are also preserved upon self-assembly, giving rise to strong absorptions for **4** and **5**.^[9a, 15, 16] The low-energy band of rectangle **4** is red-shifted with respect to that of acceptor **2** by ~ 10 nm. Similar red-shifts are observed for bands in **5** that correspond to absorptions of donor **3**.

The emission behaviour of rectangle **5** was studied at room temperature in methanol solutions, revealing bands at 525 and 561 nm upon excitation at 390 nm. The fact that the emission wavelengths of **5** match well with those of the acceptor **3**, indicates that the emission also originates from the arene–Ru moiety (Figure 4). The emission intensity of **5** was significantly quenched at the same molar concentrations as that of the acceptor **3**. The intramolecular photo-induced electron transfer (PET) in **5**, plausibly from the amide donor to the arene–Ru moiety was fully blocked in the presence of anions and **5**. Because electron transfer in PET indicates the direction from a donor **1** to an acceptor **3**, as also observed in other supramolecular systems.^[9a, 15, 22]

Colorimetric sensing of anions

The ability of rectangle **5** to act as an anion sensor was initially evidenced by visual examination of methanol solutions (1×10^{-5} M concentration) before and after anion addition. Tetrabutylammonium (TBA) salts of F^- , Cl^- , PF_6^- , and NO_3^- and sodium salts of AcO^- , BzO^- , di-oxalate, di-tartrate, and tri-citrate ions were used as analytes. The photograph in Figure 5 shows the colour of **5** under UV irradiation in the presence of oxalate, tartrate, and citrate ions, whereas the mono-anions F^- , Cl^- , PF_6^- , NO_3^- , AcO^- , and BzO^- , induce almost no colour change. Observation of this strong interaction between the receptor and multi-carboxylate anions over mono-anions motivated a quantitative investigation of the system.

UV-Vis absorption titration study

Anion sensing by rectangle **5** was achieved by observing the spectral changes of methanol solutions upon addition of the analyte. As shown in Figure 6, the absorption profile of **5** is largely invariant to the presence of 4 equiv of mono-anions, such as F^- , Cl^- , PF_6^- , NO_3^- , AcO^- , and BzO^- . On the other hand, the absorption spectra changed significantly upon addition of multi-carboxylates, indicating a strong interaction between the receptors and the anions. Since the amide donors of **5** can provide cooperative geometric assistance to selectively host multi-carboxylate anions via H-bonding, such interactions can account for the colour changes shown in Figure 5.

In order to further quantify the sensor-anion interaction, spectrophotometric titrations were carried out with oxalate, citrate, and tartrate ions. Upon addition of an aqueous solution of tartrate, the strong absorptions of **5** at 612 and 566 nm decreased in intensity while new absorptions at 516 and 480 nm gradually increased, reaching maxima at 4.0 equiv of tartrate anion.

The presence of two clear isosbestic points at 440 and 540 nm implies the formation of hydrogen bonding between the amide donor and the tartrate anion (Figure 7). Moreover, the absorbances at 390, 450 and 650 nm remained constant in the presence of more than 1 equiv of tartrate anions, indicating the formation of a 1:1 complex between **5** and the tartrate anions. A Job plot (see the Supporting Information) confirms that binding occurs in a 1:1 stoichiometry of tartrate and **5**, consistent with the analyte either binding to both amide groups, or binding to a single group such that a second tartrate is blocked from interacting with the remaining amide. A binding constant (K) of $5.5 \times 10^4 M^{-1}$ in methanol was determined based on the 1:1 binding isotherm.

The binding efficiency of **5** towards biologically relevant oxalate and citrate anions was also studied via titration studies, resulting in K values of $3.0 \times 10^3 \text{ M}^{-1}$ for oxalate and $3.7 \times 10^4 \text{ M}^{-1}$ for citrate (Figure 8). All three titration studies support a strong binding interaction between the multi-carboxylate anions and **5**.

Fluorescence titration study

The fluorescence behaviour of **5** shows similar selective sensitivity to anions as was seen in the absorption experiments. That is, the emission profile of **5** undergoes nominal changes upon the addition of an excess of a variety of mono anions, such as F^- , Cl^- , PF_6^- , NO_3^- , AcO^- , and BzO^- (Figure 9, $\lambda_{\text{ex}} = 390 \text{ nm}$). In contrast to these small intensity changes, there was a large increase in both the 525 nm and 561 nm emission bands of **5** upon addition of aqueous solutions of multi-carboxylate anions. As such, photoluminescence titrations of **5** with multi-carboxylate anions were carried out in analogy to the spectrophotometric measurements.

Fluorescence titration studies confirmed the preferential binding of multi-carboxylate anions via photoluminescence (PL) titrations which showed an approximate 10-fold increase in fluorescence upon gradual addition of tartrate. These findings established that rectangle **5** could be used as a turn-on sensor for such anions.

Similar titration results were obtained for oxalate and citrate in methanol, with high fluorescence enhancement (see Figure 11). The large binding constants and high fluorescence enhancement indicate significant interactions between these anions and rectangle **5**.

The observed increase in emission may be due to an attenuation of PET from the arene–Ru fluorophore to the receptor when a hydrogen bond is formed between the amides of **5** and a dicarboxylate analyte. Since this PET is a quenching pathway, such hydrogen bonding would intensify fluorescence. The large increase in fluorescence upon multi-carboxylate anion binding is particularly interesting because species showing such behaviour may act as a new type of turn-on fluorescent chemosensor for detecting biologically important anions, including oxalate, tartrate, and citrate.

^1H NMR titration study

In order to understand the binding interaction of **5** with anions, ^1H NMR titration experiments between **5** and oxalate were carried out. To avoid solubility problems associated with sodium oxalate, the ^1H NMR titration studies were performed with the TBA salt of the oxalate anion (see the Supporting Information S4). The NH proton peak for **5** appeared at δ 9.90 ppm in acetone- d_6 . The intensity of the peak decreased upon addition of 0.5 equiv of oxalate, and completely disappeared after adding 1.0 equiv of oxalate anion. These results suggest the 1:1 binding between the amidic-NH and oxalate anion.

Selectivity experiments

Selectivity studies of **5** towards tartrate over other anions were carried out by adding a mixture of 4 eq. of tartrate and competing anions to a solution of **5** in methanol (Figure 12). In all cases, the presence of tartrate significantly increased the fluorescent emission relative to free **5** and mixtures containing only the competing anions. The high selectivity for tartrate over other anions which manifests in increased fluorescence confirms that such receptors have potential for use as multi-carboxylate sensors.

Conclusion

We synthesized two new tetranuclear rectangles by coordination-driven self-assembly between two different arene-Ru-based acceptors and an asymmetrical amide donor ligand. These rectangles were characterized by multinuclear ^1H NMR and ESI-MS spectroscopy. The solid-state structure of **5** was confirmed by single crystal diffraction studies. UV-Vis and fluorescence studies were carried out, and the luminescence of rectangle **5** was determined to be selectively sensitive to biologically important multi-carboxylate anions. The anion sensing behavior was attributed to the attenuation of a PET quenching pathway present in **5**. Blocking PET from the arene-Ru moiety to the amidic donor in **5** upon binding of specific anions to metalla-rectangle **5** provided turn-on emission characteristics. These results suggest that rectangle **5** binds oxalate, citrate, and tartrate anions selectively and strongly in methanol, whereas mono-anions interact only weakly. We believe that this approach will provide new insights into designing specific multi-carboxylate sensors that could be biologically and chemically important.

Experimental Section

Materials and methods

All chemicals used in this work were purchased from commercial sources and used without further purification. The starting arene-ruthenium chlorides^[18e, 20] and ligand^[16] were prepared as previously described. ^1H and ^{13}C NMR spectra were recorded on a Bruker 300 MHz NMR spectrometer. ^1H NMR chemical shifts are reported relative to residual solvent signals. Mass spectra were recorded on a Micromass Quattro II triple-quadrupole mass spectrometer using electrospray ionization (ESI) running the MassLynx software suite. Elemental analyses were performed using an Elemental GmbH Vario EL-3 instrument. Absorption spectra were recorded using a CARY 100 Conc UV-Visible spectrophotometer. Fluorescence titration studies were carried out on a HORIBA FluoroMax-4 fluorometer.

UV-Vis anion binding study

A stock solution of **5** in CH_3OH (2.0 mL, 1×10^{-5} M) was prepared and placed in a quartz cell. Stock solutions (1×10^{-3} M) of the corresponding anions in water were added incrementally and the absorption spectra were recorded at room temperature. The results show that **5** forms a 1:1 receptor-anion adduct with the oxalate anion. The binding constant (K) of the host-guest complex was determined by fitting the experimental data to a 1:1 binding isotherm.

Fluorescence sensing study

A 2 mL stock solution (1×10^{-5} M) of rectangle **5** was placed in a 1 cm wide quartz cell, and anion stock solutions (1×10^{-3} M) were added incrementally. A series of aqueous solutions of 1×10^{-3} M of tetrabutylammonium salts of F^- , Cl^- , CH_3COO^- , PF_6^- , and NO_3^- , and sodium salts of benzoate, oxalate, tartrate, and citrate were prepared. The titration experiments were carried out at 298 K, and each measurement was repeated at least three times to get concordant values. Both the excitation and emission slits were 5 nm. An excitation wavelength of 390 nm (λ_{exc}) was used for all measurements, and emission was monitored at 525 and 561 nm.

X-ray crystallography for **5**

The diffraction data from a single crystal of **5** mounted on a loop were collected at 100 K on an ADSC Quantum 210 CCD diffractometer with a synchrotron radiation source ($\lambda = 0.80000 \text{ \AA}$) at Macromolecular Crystallography Beamline 6B1, Pohang Accelerator Laboratory (PAL), Pohang, Korea. The raw data were processed and scaled using the

HKL2000 program. The structure was solved by direct methods, and refinements were carried out with full-matrix least-squares on F^2 with appropriate software in the SHELXTL package. All non-hydrogen atoms were refined anisotropically. Hydrogen atoms were added to their geometrically ideal positions, except on the hydroxyl group of alcohol. The crystallographic data are summarized in Table S1. CCDC 880535 contains the supplementary crystallographic data for this paper. These data can be obtained free of charge from The Cambridge Crystallographic Data Centre via www.ccdc.cam.ac.uk/data_request/cif.

General Synthetic Method for 4 and 5

A mixture of starting complex **2** or **3** (0.1 mmol) and 2 equiv of AgCF_3SO_3 (0.2 mmol) in methanol was stirred at room temperature for 2 h and filtered to remove AgCl . The corresponding donor ligand **1** (0.1 mmol) was added to the filtrate. The mixture was then stirred at room temperature for 12 h, and the solvent was removed under reduced pressure. The residue was taken up in acetone, the extract was filtered and concentrated, and the product was precipitated by adding diethyl ether and collected.

Synthesis of molecular rectangle 4

Red crystalline solid in 91% yield. Analytically calculated for $\text{C}_{94}\text{H}_{86}\text{F}_{12}\text{N}_6\text{O}_{22}\text{Ru}_4\text{S}_4$: C, 46.80%; H, 3.59%; N, 3.48%; S, 5.32; Found: C, 46.87%; H, 3.72%; N, 5.60%; S, 5.21%. MS (ESI) calculated for $[\text{M} - 2\text{OTf}]^{2+}$ m/z 1057.1, found 1057.1; calculated for $[\text{M} - 3\text{OTf}]^{3+}$ m/z 655.4, found 655.6. ^1H NMR (Nitromethane- d_3 , 300 MHz, δ , ppm): 9.49 (s, 2H, CONH), 9.19 (s, 2H, CONH), 8.49–8.44 (m, 8H, H_a/H_a'), 8.25–8.23 (m, 8H, H_f/H_f'), 8.23–7.22 (m, 8H, H_b/H_b'), 7.88–7.81 (m, 8H, H_c/H_c'), 7.75–7.71 (m, 8H, H_e/H_e'), 7.46–7.43 (m, 8H, H_d/H_d'), 5.99–5.96 (m, 16H; $-\text{C}_6\text{H}_4$), 5.79–5.77 (m, 16H, $-\text{C}_6\text{H}_4$), 7.57–7.56 (m, 8H, H_{ar}), 2.93–2.85 (m, 8H, $-\text{CH}(\text{CH}_3)_2$), 2.11 (s, 24H; $-\text{CH}_3$), 1.38–1.34 (m, 48H; $-\text{CH}(\text{CH}_3)_2$).

Synthesis of molecular rectangle 5

Green crystalline solid in 92% yield. Analytically calculated for $\text{C}_{118}\text{H}_{98}\text{F}_{12}\text{N}_6\text{O}_{22}\text{Ru}_4\text{S}_4$: C, 52.25%; H, 3.64%; N, 3.10%; S, 4.73; Found: C, 52.37%; H, 3.72%; N, 5.40%; S, 4.51%. MS (ESI) calculated for $[\text{M} - 3\text{OTf}]^{3+}$ m/z 755.4, found 755.6. ^1H NMR (Nitromethane- d_3 , 300 MHz, δ , ppm): 9.19 (s, 2H, CONH), 8.88 (s, 2H, CONH), 8.79–8.76 (m, 8H, H_a/H_a'), 8.74–8.76 (m, 8H, H_f/H_f'), 8.57–8.51 (m, 16H, H_{ar}), 7.97–7.92 (m, 16H, H_{ar}), 7.70–7.65 (m, 8H, H_b/H_b'), 7.61–7.56 (m, 8H, H_c/H_c'), 7.33–7.30 (m, 8H, H_e/H_e'), 7.29–7.26 (m, 8H, H_d/H_d'), 5.98–5.94 (m, 16H; $-\text{C}_6\text{H}_4$), 5.77–5.72 (m, 16H, $-\text{C}_6\text{H}_4$), 3.07–3.00 (m, 8H, $-\text{CH}(\text{CH}_3)_2$), 2.28 (m, 24H; $-\text{CH}_3$), 1.39–1.36 (m, 48H; $-\text{CH}(\text{CH}_3)_2$).

Supplementary Material

Refer to Web version on PubMed Central for supplementary material.

Acknowledgments

We gratefully acknowledge generous financial support from the World Class University (WCU) program (R33-2008-000-10003) and Priority Research Centers program (2009-0093818) through the National Research Foundation of Korea (NRF) funded by the Ministry of Education, Science and Technology. P.J.S. thanks the National Institutes of Health (NIH), USA (Grant GM-057052) for financial support. X-ray diffraction experiments using synchrotron radiation were performed at the Pohang Accelerator Laboratory in Korea.

References

1. a) Yoon J, Kim SK, Singh NJ, Kim KS. *Chem Soc Rev.* 2006; 35:355. [PubMed: 16565752] b) Beer PD, Gale PA. *Angew Chem.* 2001; 113:502. *Angew Chem Int Ed.* 2001; 40:486. c) Schraderr, T.; Hamilton, AD., editors. *Functional Synthetic Receptors.* Wiley-VCH; Weinheim: 2005. d) Ilioudis CA, Steed JW. *J Supramol Chem.* 2001; 1:165. e) Llinares JM, Powell D, Bowman-James K. *Coord Chem Rev.* 2003; 240:57. f) Bondy CR, Loeb SJ. *Coord Chem Rev.* 2003; 240:77. g) Gale PA. *Coord Chem Rev.* 2001; 213:79. h) Sessler, JL.; Gale, PA.; Cho, WS. *Anion Receptor Chemistry.* Royal Society of Chemistry; Cambridge: 2006. i) Sessler JL, Camilo S, Gale PA. *Coord Chem Rev.* 2003; 240:17. j) Gale PA. *Chem Commun.* 2005:3761.
2. Selected reviews for anion binding: Stibor I. *Anion Sensing.* Topics in Current Chemistry. Springer-Verlag Berlin 2005:255, 238. Vilar R. *Recognition of Anions. Structure and Bonding.* Springer-Verlag Berlin 2008. Rehm TH, Schmuck C. *Chem Soc Rev.* 2010; 39:3597. [PubMed: 20552123] Quang DT, Kim JS. *Chem Rev.* 2007; 107:3780. [PubMed: 17711335] Pu L. *Chem Rev.* 2004; 104:1687. [PubMed: 15008630]
3. (a) Robertson WG, Hughes H. *Scanning Microsc.* 1993; 7:391. [PubMed: 8316808] b) Morakot N, Rakrai W, Keawwangchai S, Kaewtong C, Wannoo B. *J Mol Model.* 2010; 16:129. [PubMed: 19521724] c) Pal R, Parker D, Costello LC. *Org Biomol Chem.* 2009; 7:1525. [PubMed: 19343236] d) Pal R, Parker D, Costello LC. *Org Biomol Chem.* 2009; 7:1525. [PubMed: 19343236] e) Costello LC, Franklin RB. *Prostate Cancer Prostatic Dis.* 2008; 12:17. [PubMed: 18591961]
4. Kasidas GP, Rose GA. *Clin Chim Acta.* 1986; 154:49. [PubMed: 3943224]
5. Skotty DR, Nieman TA. *J Chromatogr B.* 1995; 665:27.
6. Jiang ZL, Zhao MX, Liao LX. *Anal Chim Acta.* 1996; 320:139.
7. a) Schell-Feith EA, Maerdijk A, van Zweiten PHT, Zanderland HM, Holscher HC, Kist-van Holthe J, von der Heijden BJ. *Pediatric Nephrol.* 2006; 21:1830. b) Cebotaru V, Kaul S, Devayst O, Cai H, Racusen L, Guggino WB, Guggino SE. *Kidney Int.* 2005; 68:642. [PubMed: 16014041]
8. a) Liu SY, Fang L, He YB, Chan WH, Yeung KT, Cheng YK, Yang RH. *Org Lett.* 2005; 7:5825. [PubMed: 16354076] b) Zeng ZY, He YB, Wu JL, Wei LH, Liu X, Meng LZ, Yang X. *Eur J Org Chem.* 2004:2888. c) Wu J-L, He Y-B, Zeng Z-Y, Wei L-H, Meng L-Z, Yang T-X. *Tetrahedron.* 2004; 60:4309. d) Kacprzak K, Gawronski J. *Chem Commun.* 2003:1532. e) Raker J, Glass TE. *J Org Chem.* 2002; 67:6113. [PubMed: 12182650] f) Linton BR, Goodman MS, Fan E, van Arman SA, Hamilton AD. *J Org Chem.* 2001; 66:7313. [PubMed: 11681943] g) Benito JM, Gomez-Garcia M, Jimenez Blanco JL, Ortiz Mellet C, Garcia Fernandez JM. *J Org Chem.* 2001; 66:1366. [PubMed: 11312968]
9. a) Vajpayee V, Song YH, Lee MH, Kim H, Wang M, Stang PJ, Chi KW. *Chem Eur J.* 2011; 17:7837. [PubMed: 21611989] b) Young MJ, Chin J. *J Am Chem Soc.* 1995; 117:10577. c) Sathish S, Narayan G, Rao N, Janardhana C. *J Fluoresc.* 2007; 17:1. [PubMed: 17160729] d) Maeda H, Ito Y. *Inorg Chem.* 2006; 45:8205. [PubMed: 16999419] e) Kacprzak K, Gawronski J. *Chem Commun.* 2003:1532. f) Dieng PS, Sirlin C. *Int J Mol Sci.* 2010; 11:3334. [PubMed: 20957098]
10. a) Lee DH, Im JH, Son SU, Chung YK, Hong JI. *J Am Chem Soc.* 2003; 125:7752. [PubMed: 12822964] b) Lee JH, Park J, Lah MS, Chin J, Hong JI. *Org Lett.* 2007; 9:3729. [PubMed: 17705498]
11. a) Caltagirone C, Gale PA. *Chem Soc Rev.* 2009; 38:520. [PubMed: 19169465] b) Gale PA, Quesada R. *Coord Chem Rev.* 2006; 250:3219. c) Oshovsky GV, Reinhoudt DN, Verboom W. *Angew Chem Int Ed.* 2007; 46:2366. d) Gale PA, Garcia-Garrido SE, Garric J. *Chem Soc Rev.* 2008; 37:151. [PubMed: 18197339] e) Suksai C, Tuntulani T. *Chem Soc Rev.* 2003; 32:192. [PubMed: 12875025] f) Sessler JL, Camilo S, Gale PA. *Coord Chem Rev.* 2003; 240:17. g) Han YF, Jia WG, Lin YJ, Jin GX. *Angew Chem Int Ed.* 2009; 48:6234. h) Bondy CR, Loeb SJ. *Coord Chem Rev.* 2003; 240:77. i) Tzeng BI, Chen YF, Wu CC, Hu CC, Chang YT, Chen CK. *New J Chem.* 2007; 31:202. j) Kubik S. *Chem Soc Rev.* 2009; 38:585. [PubMed: 19169467] k) Hua Y, Flood AH. *Chem Soc Rev.* 2010; 39:1262. [PubMed: 20349532] l) O'Neil EJ, Smith BD. *Coord Chem Rev.* 2006; 250:3068. m) Gunnlaugsson T, Glynn M, Tocci GM, Kruger PE, Pfeffer FM. *Coord Chem Rev.* 2006; 250:3094. n) Rice CR. *Coord Chem Rev.* 2006; 250:3190.
12. Anslin EV. *J Org Chem.* 2007; 72:687. [PubMed: 17253783]

13. a) Fabbrizzi L, Licchelli M, Taglietti AJ. *Chem Soc Dalton Trans.* 2003;3471.b) de Silva AP, Gunaratne HQN, Gunnlaugsson T, Huxley AJM, McCoy CP, Rademacher JT, Rice TE. *Chem Rev.* 1997; 97:1515. [PubMed: 11851458] c) Martínez-Máñez R, Sancenón F. *Chem Rev.* 2003; 103:4419. [PubMed: 14611267] d) Martínez-Máñez R, Sancenón F. *J Fluoresc.* 2005; 15:267. [PubMed: 15986153]
14. a) Adarsh NN, Tocher DA, Ribas J, Dastidar P. *New J Chem.* 2010; 34:2458.b) Kumar A, Sun SS, Lees AJ. *Coord Chem Rev.* 2008; 252:922.c) Sun SS, Lees AJ. *Chem Commun.* 2000:1687.d) Kavallieratos K, de Gala SR, Austin DJ, Crabtree RH. *J Am Chem Soc.* 1997; 119:2325.e) Kavallieratos K, Bertao CM, Crabtree RH. *J Org Chem.* 1999; 64:1675. [PubMed: 11674235] f) Smith BD, Hughes MP. *J Org Chem.* 1997; 62:4492. [PubMed: 11671780]
15. Mishra A, Vajpayee V, Kim H, Lee MH, Jung H, Wang M, Stang PJ, Chi K-W. *Dalton Trans.* 2012; 41:1195. [PubMed: 22116403]
16. Mishra A, Jung H, Park JW, Kim HK, Kim H, Stang PJ, Chi KW. *Organometallics.* 2012; 31:3519. [PubMed: 22639481]
17. a) Sumbly CJ, Hanton LR. *Tetrahedron.* 2009; 65:4681.b) Yamnitz CR, Negin S, Carasel IA, Winter RK, Gokel GW. *Chem Commun.* 2010; 46:2838.c) Dorazco-González A, Höpfl H, Medrano F, Yatsimirsky AK. *J Org Chem.* 2010; 75:2259. [PubMed: 20201487] d) Zhang ZH, Chen SC, Mi JL, He MY, Chen Q, Du M. *Chem Commun.* 2010; 46:8427.
18. a) Chakrabarty R, Mukherjee PS, Stang PJ. *Chem Rev.* 2011; 111:6810. [PubMed: 21863792] b) Wang M, Vajpayee V, Shanmugaraju S, Zheng YR, Zhao Z, Kim H, Mukherjee PS, Chi KW, Stang PJ. *Inorg Chem.* 2011; 50:1506. [PubMed: 21214171] c) Northrop BH, Zheng YR, Chi KW, Stang PJ. *Acc Chem Res.* 2009; 42:1554. [PubMed: 19555073] d) Mishra A, Kaushik NK, Verma AK, Gupta R. *Eur J Med Chem.* 2008; 43:2189. [PubMed: 17959275] e) Mishra A, Ali A, Upreti S, Gupta R. *Inorg Chem.* 2008; 47:154. [PubMed: 18072765] f) Mishra A, Ali A, Upreti S, Whittingham MS, Gupta R. *Inorg Chem.* 2009; 48:5234. [PubMed: 19445471] g) Mishra A, Ravikumar S, Hong SH, Kim H, Vajpayee, Lee V, Ahn HW, Wang BC, Stang M, Chi PJ, K-W. *Organometallics.* 2011; 30:6343. [PubMed: 22180697]
19. a) Vajpayee V, Yang YJ, Kang SC, Kim H, Kim IS, Wang M, Stang PJ, Chi KW. *Chem Commun.* 2011; 47:5184.b) Barry NPE, Govindaswamy P, Furrer J, Süß-Fink G, Therrien B. *Inorg Chem Commun.* 2008; 11:1300.c) Barry NPE, Austeri M, Lacour J, Therrien B. *Organometallics.* 2009; 28:4894.d) Barry NPE, Zava O, Furrer J, Dyson PJ, Therrien B. *Dalton Trans.* 2010; 39:5272. [PubMed: 20442944] e) Therrien B, Süß-Fink G, Govindaswamy P, Renfrew AK, Dyson PJ. *Angew Chem Int Ed.* 2008; 47:3773.f) Shanmugaraju S, Bar AK, Joshi SA, Patil YP, Mukherjee PS. *Organometallics.* 2011; 30:1951.g) Linares F, Galindo MA, Galli S, Romero MA, Navarro JAR, Barea E. *Inorg Chem.* 2009; 48:7413. [PubMed: 19586019] h) Han YF, Jia WG, Yu WB, Jin GX. *Chem Soc Rev.* 2009; 38:3419. [PubMed: 20449060] i) Gao J, Rochat S, Qian X, Severin K. *Chem Eur J.* 2010; 16:513.j) Kilbas B, Mirtschin S, Scopelliti R, Severin K. *Chem Sci.* 2012; 3:701.k) Pitto-Barry A, Barry NPE, Zava O, Deschenaux R, Dyson PJ, Therrien B. *Chem Eur J.* 2011; 17:1966. [PubMed: 21274948] l) Thomas JA. *Dalton Trans.* 2011; 40:12005. [PubMed: 21986864]
20. Barry NPE, Furrer J, Therrien B. *Helv Chim Acta.* 2010; 93:1313.
21. Zhang Q, He L, Liu JM, Wang W, Zhang J, Su CY. *Dalton Trans.* 2010; 39:11171. [PubMed: 20967343]
22. Shanmugaraju S, Bar AK, Chi KW, Mukherjee PS. *Organometallics.* 2010; 29:2971.

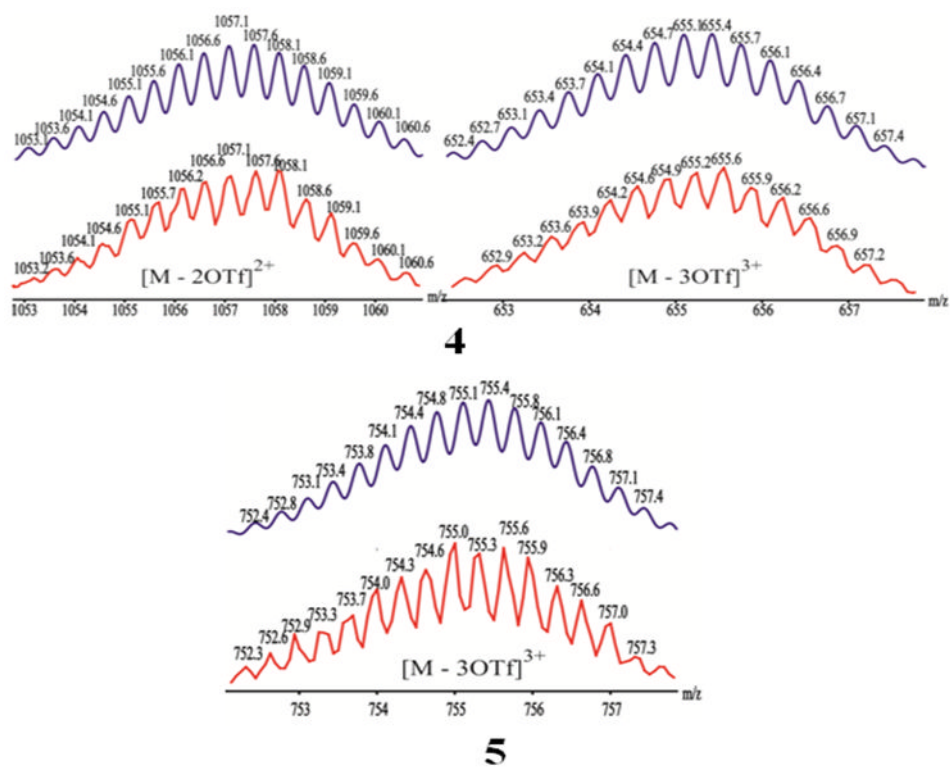


Figure 1. Theoretical (top) and experimental (bottom) ESI-MS results for self-assembled [2+2] rectangles **4** and **5**.

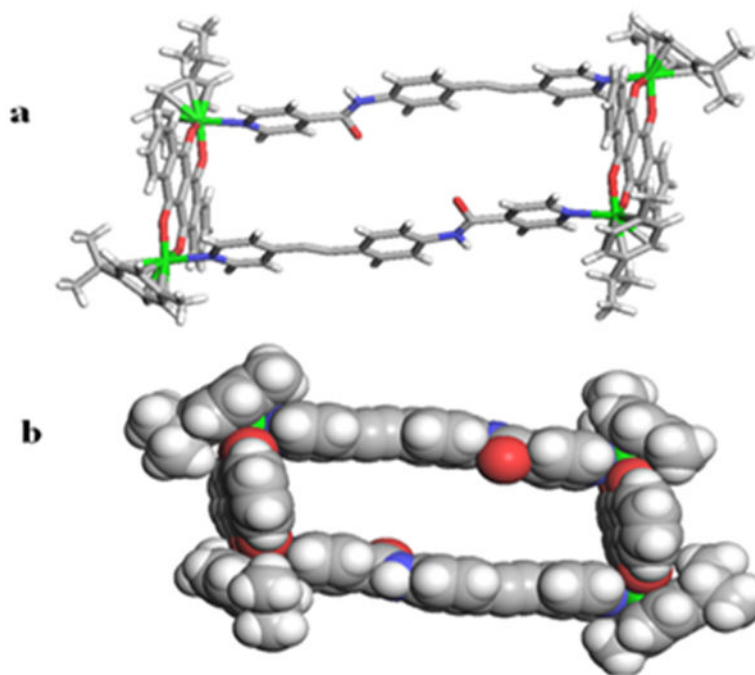


Figure 2. (a) X-ray crystal structure of rectangle **5** with four Ru²⁺ ions (green) coordinated by four pyridyl N atoms (blue). (b) Space-filling CPK model of rectangle **5** in head-to-tail orientation. Hydrogen atoms and counter anions omitted for clarity.

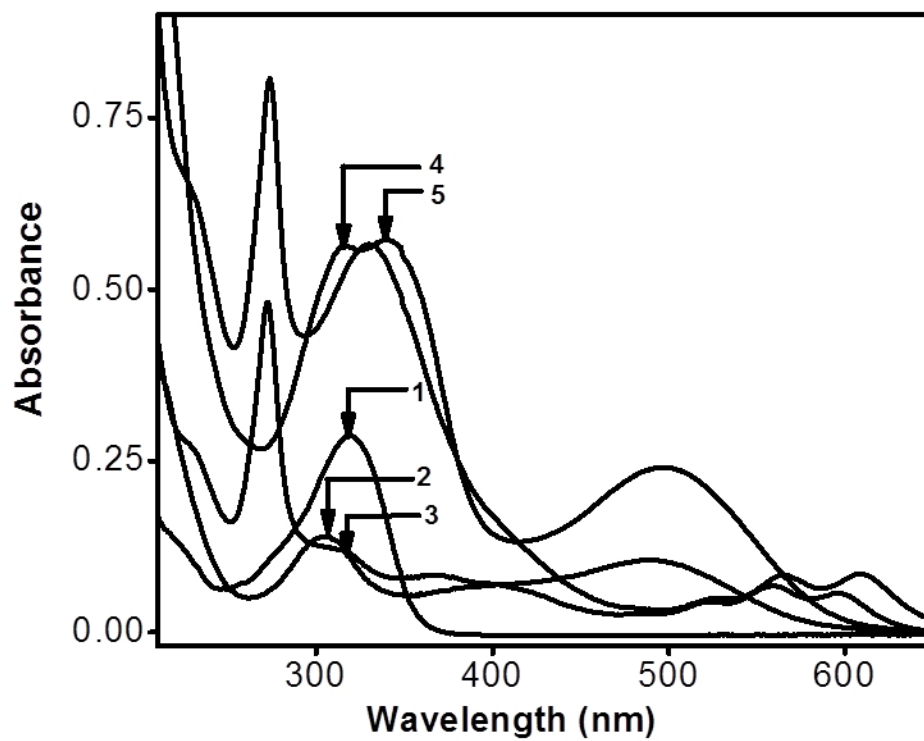


Figure 3.
Electronic absorption spectra of 1–5 in methanol.

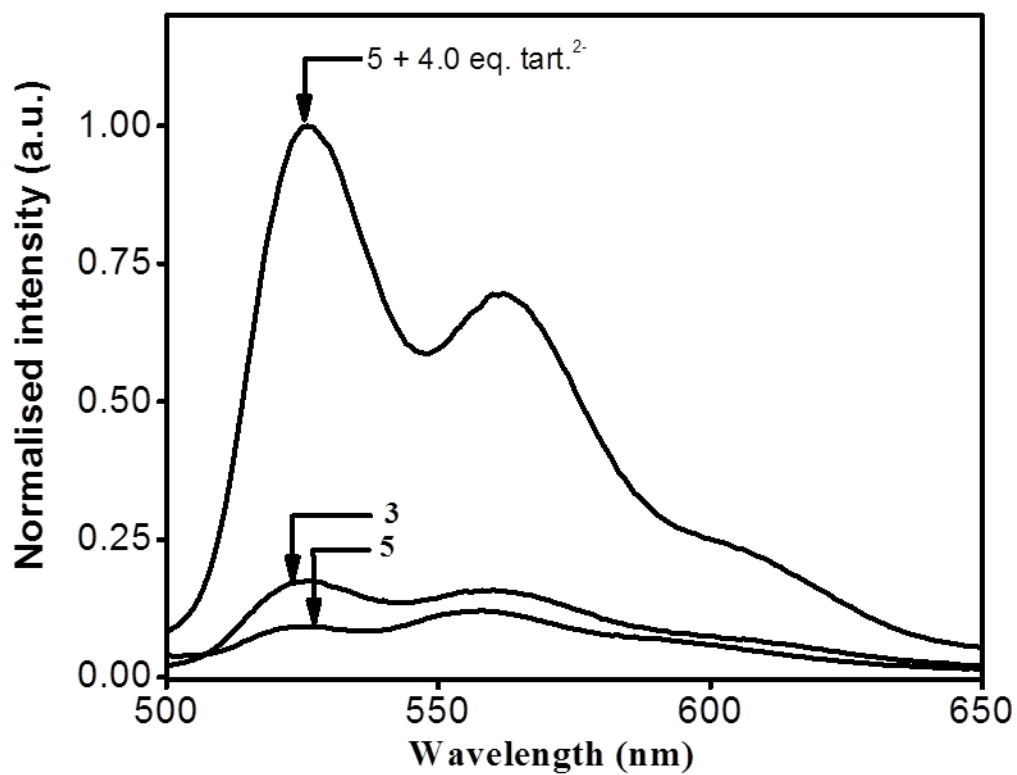


Figure 4. Normalized emission spectra of **3**, **5** and mixture of 4.0 eq. of oxalate anion and **5** (*blue*) in methanol.

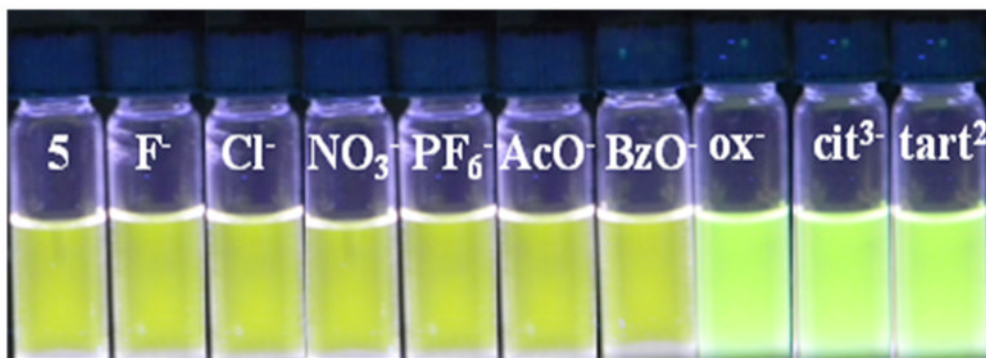


Figure 5. Photograph showing the emission intensity changes of solutions of **5** in methanol in the presence of 4.0 eq. of various anions.

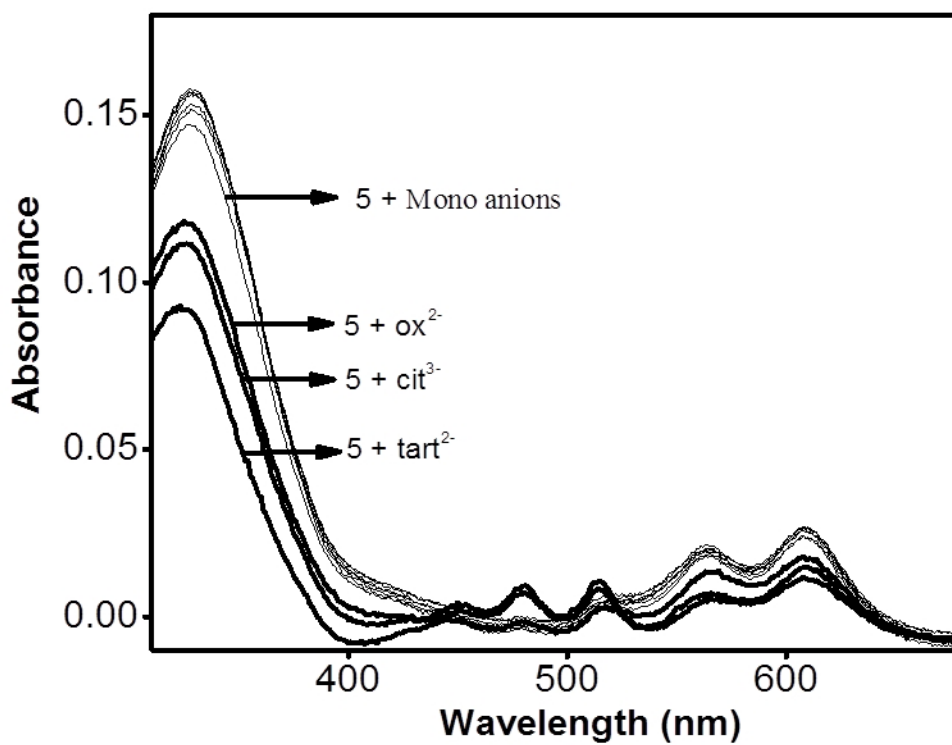


Figure 6. Changes in the absorption spectra of **5** in methanol (1×10^{-5} M) upon adding 4.0 equiv. of an aqueous solution (1×10^{-3} M) of TBA salts (F^- , Cl^- , NO_3^- , and PF_6^-) and sodium salts [AcO^- , BzO^- , di-oxalate (ox^{2-}), tri-citrate (cit^{3-}), di-tartrate ($tart^{2-}$)].

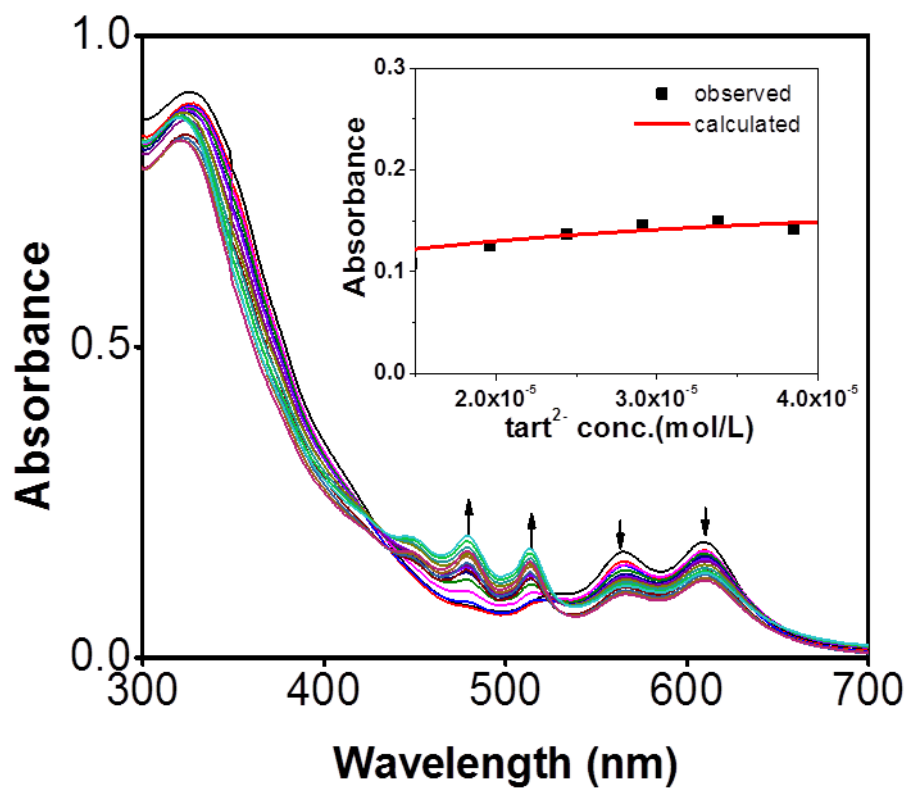


Figure 7. Changes in the absorption spectra of **5** upon incremental addition of tartrate anion in methanol. Inset: 1:1 binding isotherm.

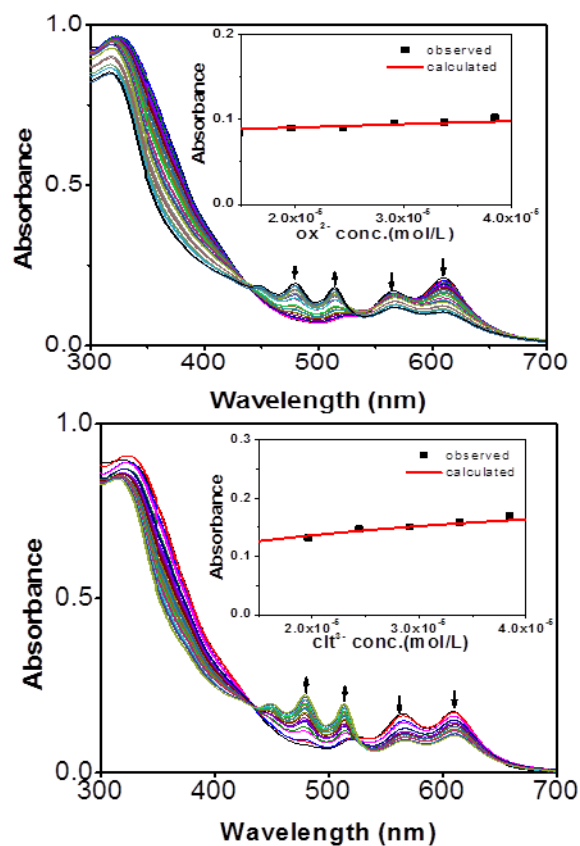


Figure 8. Changes in the absorption spectra of **5** in methanol (1×10^{-5} M) upon incremental addition of oxalate anion (*top*) and citrate anion (*bottom*). Insets: 1:1 binding curves; ox²⁻ = di-sodium oxalate, cit³⁻ = tri-sodium citrate.

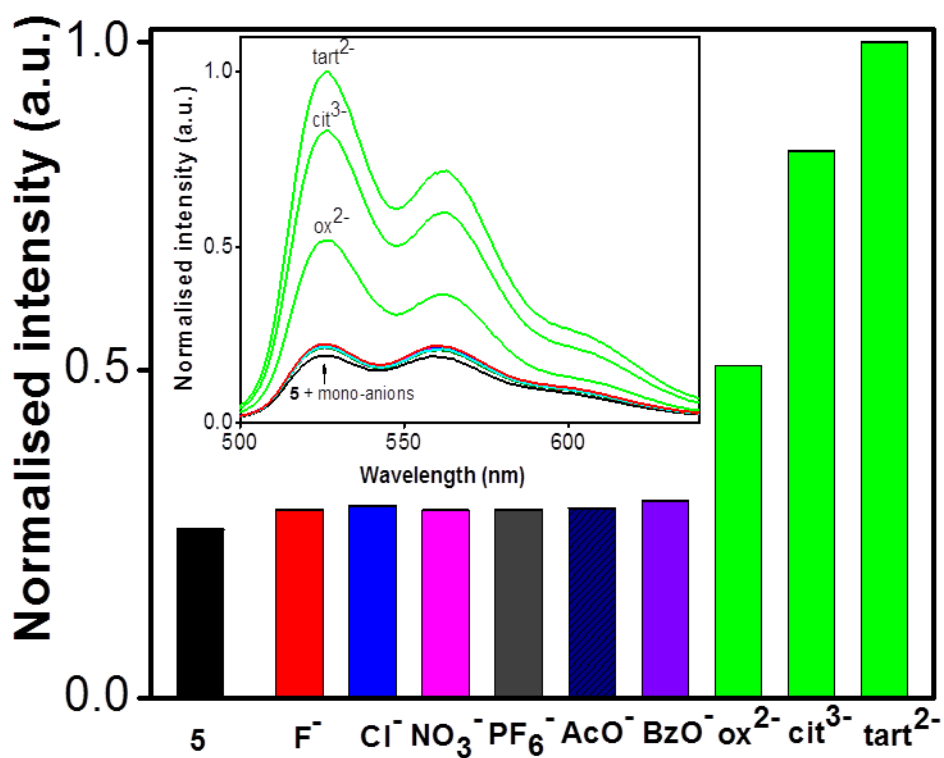


Figure 9. Changes in the emission spectra of **5** in methanol (1×10^{-5} M) upon adding 4.0 equiv. of an aqueous solution (1×10^{-3} M) of TBA salts; F⁻, Cl⁻, NO₃⁻, and PF₆⁻ and sodium salts of AcO⁻, BzO⁻, di-oxalate (ox²⁻), tri-citrate (cit³⁻), di-tartrate (tart²⁻), ions.

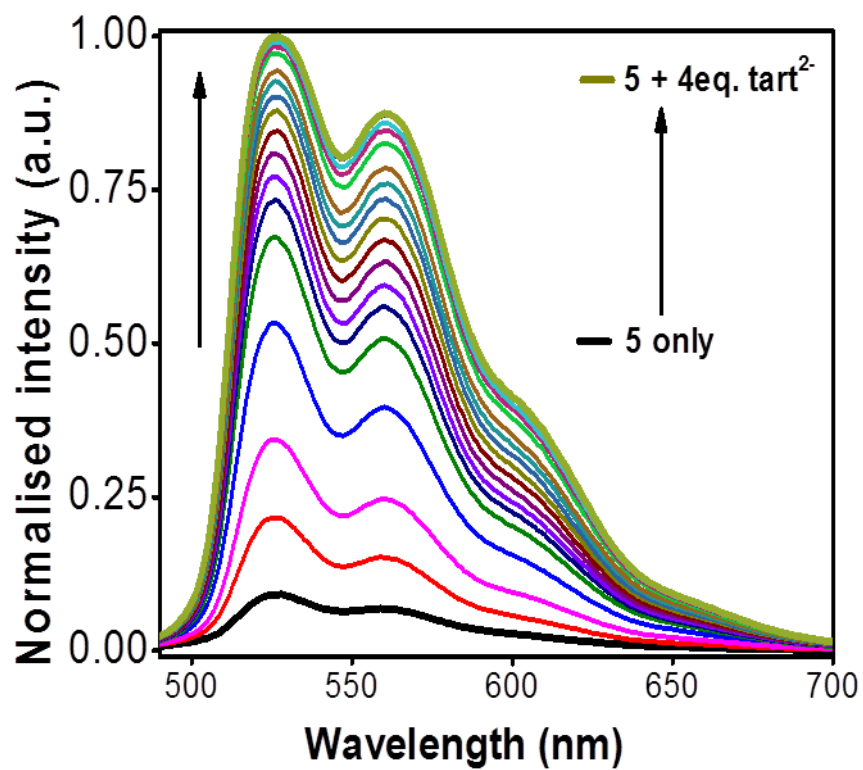


Figure 10. Changes in the emission spectra of **5** upon incremental addition of tartrate anion in methanol.

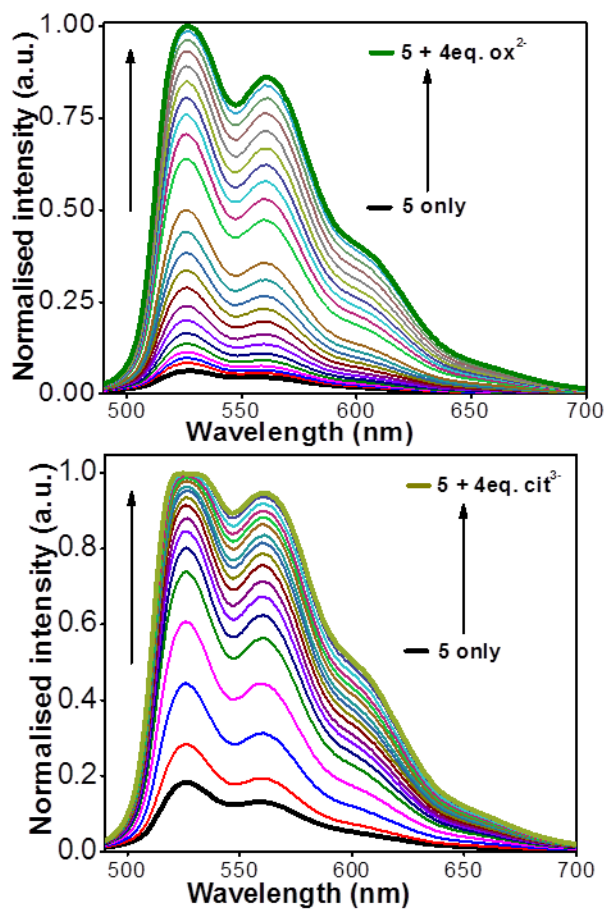


Figure 11. Changes in the emission spectra of **5** in methanol (1×10^{-5} M) upon incremental addition of oxalate (*top*) and citrate anion (*bottom*).

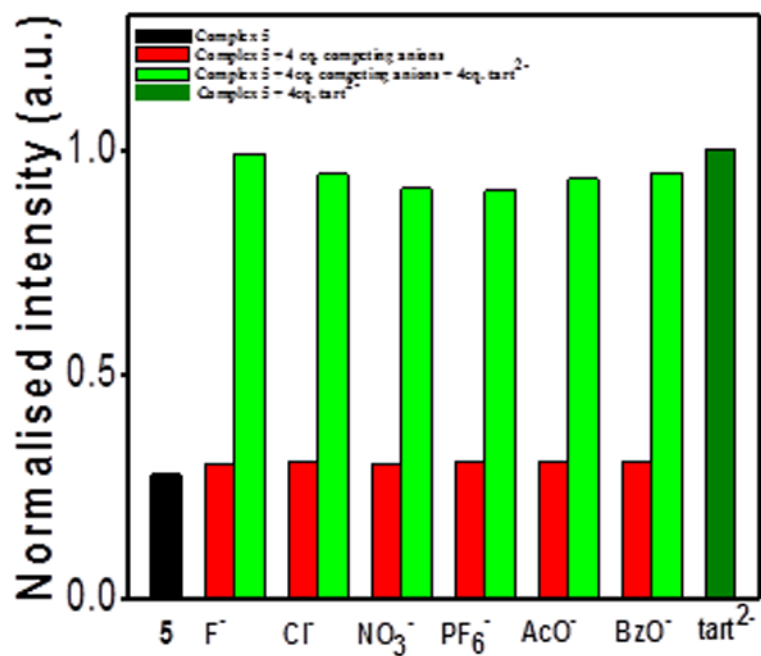
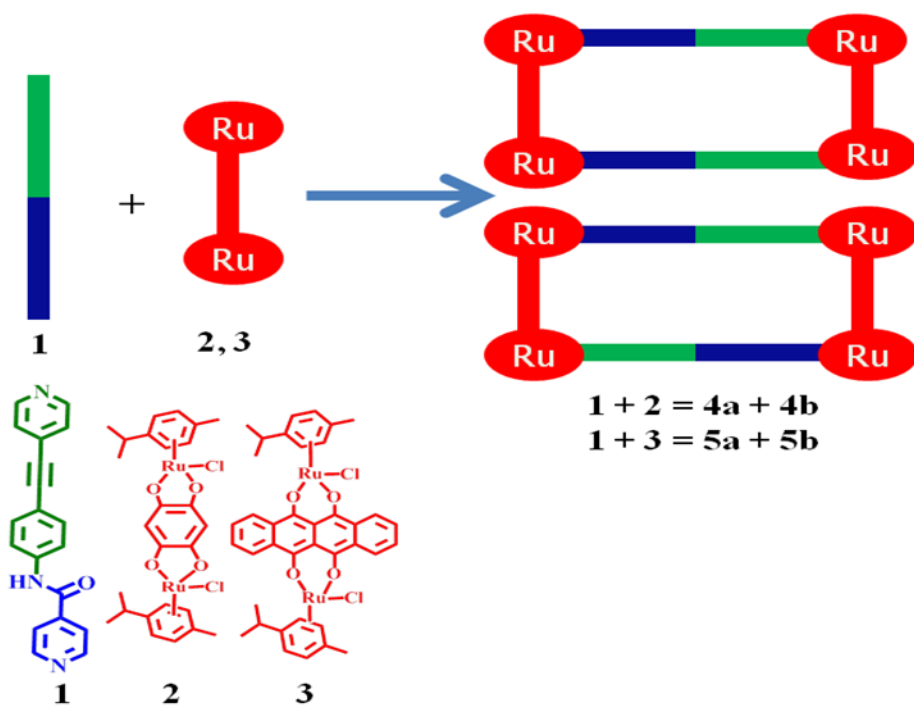


Figure 12. Selectivity studies of **5** with tart²⁺ in the presence of other anions.



Scheme 1.
Synthesis of molecular rectangles **4** and **5**.